The Effects of Privacy Protection on Forecast Accuracy

1. Introduction

Forecasting is popular in a variety of fields, such as consumer analytics, renewable energy and power industries, and census tracking, all of which may benefit from the use of commercially or personally sensitive data. Examples include using data from smart devices (Boone et al., 2019) and collaboratively shared power generation data (Gonçalves et al., 2021) to improve forecast accuracy. The privacy concerns associated with sensitive data have been demonstrated across many domains. Data ranging from consumer locations (de Montjoye et al., 2013) to smart meter usage (Véliz & Grunewald, 2018) can be used to identify individuals and/or infer sensitive information about them. Furthermore, a large number of privacy laws such as the General Data Protection Regulation (GDPR)[1] require organizations to protect their sensitive data to avoid fines, and place strict limitations on data transfers and processing[2].

These legal limitations can be circumvented when data is properly anonymized[3]. For example, during the COVID-19 pandemic, mobile phone position data was anonymized through aggregation to origin-destination matrices, which were used to study population mobility patterns in the EU (Santamaria et al. 2020). This data was subsequently used in nowcasting GDP during the COVID-19 pandemic (Barbaglia 2020). Data that is not anonymous, on the other hand, is subject to purpose limitation, and cannot be freely re-used[4]. In addition to legal compliance, other reasons for protecting data include reducing consumers' privacy concerns (Martin et al., 2017) or attempting to gain a competitive advantage through privacy-conscious brand positioning (Goldfarb & Tucker, n.d.). Several of the largest tech companies in the world, including IBM, Google[5], Meta, and Microsoft[6] implement various approaches to privacy protection and provide open-source code to enable others to do the same. Notably, Apple has positioned themselves as a privacy-focused company[7].

Various data protection approaches are available depending on whether time series are stored in a single data set (centralized) or spread across multiple data owners/data sets (decentralized). In the decentralized scenario, multi-party computation or federated learning enable privacy-preserving collaborative forecasting to ensure accurate forecasts while protecting sensitive data (Gonçalves et al., 2021; Goncalves, Bessa, et al., 2021; Sommer et al., 2021). We focus on the centralized scenario in which a single data owner uses privacy methods to protect a time series data set. These privacy methods alter the sensitive data to produce protected time series which limit the ability of a bad actor to identify data subjects and learn sensitive information about them. One example is the Census' use of random noise to perturb the individual and business level data that goes into calculating Quarterly Workforce Indicator data (Abowd et al., 2012). The concern for forecasters is that privacy methods can drastically alter time series features which can significantly affect forecast accuracy., ~~leading to privacy adjusted forecasts.~~ ~~Empirical evidence of the effects of privacy~~

[1] For examples in the United States, see this map.

[2] See articles 6, 45, and 46 of the GDPR.
[3] See the description of anonymous information given in Recital 26 of the GDPR.
[4] See article 5(b) of the GDPR.
[5] See several python libraries including PipelineDP and PyDP.
[6] See the OpenDP project.
[7] See descriptions of Apple's privacy features.

Consider the example shown in Figure 1. The series shown in the middle plot is a simulated AR(1) process with autoregressive parameter $\phi_1 = 0.8$. The series on the left is the original series with random noise added to each period that is proportional to the standard deviation of the original series. Estimating an ARIMA(1, 0, 0) model on the original series yields an estimate of $\widehat{\phi_1} = 0.73$, while the noised series yields an estimate of $\widehat{\phi_1} = 0.16$. The series on the right was created by swapping the original series values with values from two other simulated AR(1) processes, both with $\phi_1 = 0.8$. The swapped series better preserves the autocorrelation of the original series, with an estimate of $\widehat{\phi_1} = 0.56$.

Figure 1: comparison of protected AR(1) processes to the original AR(1) process.

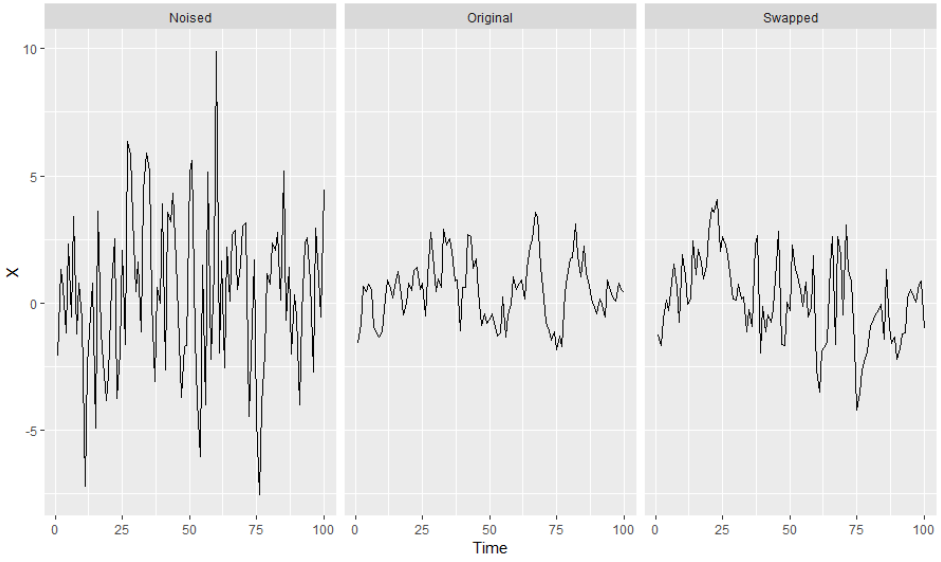

This paper examines how data protection changes time series features and how this affects forecasting model performance.
First, we investigate the drivers of changes in forecast accuracy for protected data. Specifically, we examine the effects of privacy protection on time series features, which provide a link to explain why privacy methods produce changes in forecast accuracy. To limit reductions in forecast accuracy that can arise from data protection, we develop a new matrix-based privacy method called *k*-nts+ which swaps the values of time series with similar features to balance the trade-off between privacy and forecast accuracy. We provide empirical results of forecast accuracy and privacy for protected data and examine model-specific behavior to understand why certain models perform better than others.

Figure 2: Framework to study the effects of privacy methods on forecast accuracy using time series features. Blue arrows indicate the flow of results which inform our proposed protection method based on swapping values of time series with similar features to limit the changes in features and forecast accuracy between the original and protected data.

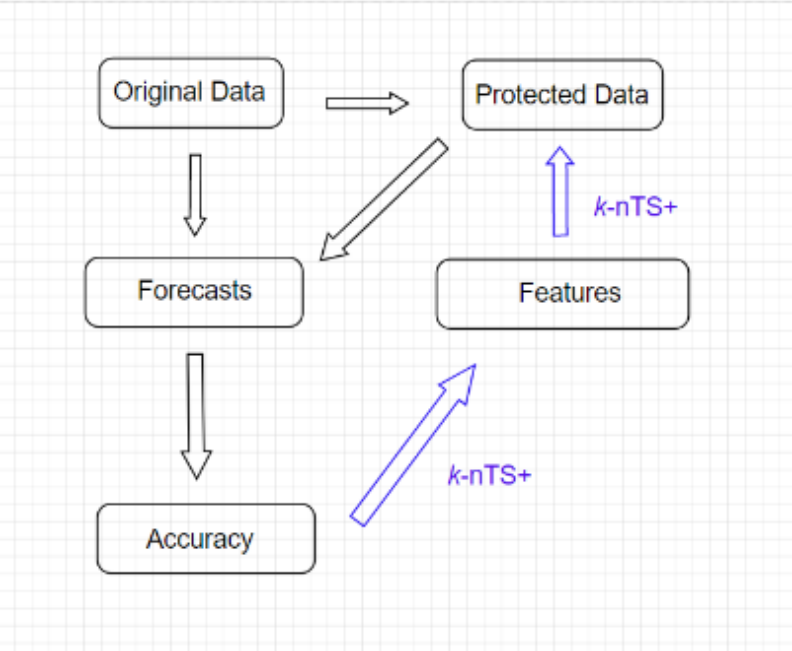

The rest of the paper proceeds as follows…

2. Lit Review

While it has been demonstrated that differential privacy degrades forecast accuracy for VAR models and recurrent neural networks (RNNs) (Gonçalves et al., 2021; Imtiaz et al., 2020), there is no work which compares how multiple forecasting models perform on protected data. This comparison is needed because different forms of data protection produce different data points which will ultimately have different forecasts than what would be produced based on the original data.

Some forecasters have studied data privacy and forecasting in the context of collaborative forecasting. (Goncalves, Pinson, et al., 2021) explored a data market where data owners are compensated for sharing their data, and purchase forecasts based on the data from other parties.

While data owners have a monetary incentive to share their data, they may be discouraged from doing so due to privacy concerns over sharing data with a central party. In such a situation, our work would help answer how forecast accuracy would be affected if the data owners applied data protection methods prior to sharing their data in the market. In the absence of a data market, other privacy-preserving solutions for collaborative forecasting include secure multi-party computation, decomposition-based methods, and data transformation techniques, all of which are succinctly described by (Gonçalves et al., 2021).

Our interest is in privacy methods which generate protected data sets. The first methods we consider, known as additive or multiplicative noise and differential privacy, are based on incorporating random noise into the data. (Gonçalves et al., 2021) show that differential privacy reduces the forecast accuracy of VAR models even under very high values of the privacy parameter ϵ (weak privacy protection). Others have also studied the application of differential privacy to time series (Imtiaz et al., 2020; Liyue Fan & Li Xiong, 2014). Additive and multiplicative noise infuse random noise in the data but without the theoretical privacy guarantees of differential privacy. While (Abowd et al., 2012) study the use of multiplicative noise, they do not offer forecast accuracy results. Through simulated data integrity attacks, however, we know that multiplicative noise reduces forecast accuracy (Luo et al., 2018).

One interesting result from (Imtiaz et al., 2020) is that differentially private data did not always produce worse forecast accuracy when forecasting individuals' health data using a recurrent neural network. Adding random noise to time series mirrors a technique used to prevent overfitting when forecasting with neural networks (Hewamalage et al., 2021, 2022). We explore whether data protection with random noise can achieve this same regularization at meaningful levels of privacy.

Another type of privacy method is generalization, where data records are generalized to create equivalence classes of identical records. This privacy method is particularly popular for tabular data. The principle of k-anonymity (Sweeney, 2002) is used to describe when every record (or time series) is identical to at least $k - 1$ other records on a pre-determined set of attributes (or time periods). (Nin & Torra, 2009) evaluate the change in forecast accuracy for simple exponential smoothing, double exponential smoothing, linear regression, multiple linear regression, and polynomial regression applied to k-anonymized data. The authors find an overall reduction in forecast accuracy even for $k = 2$ but do not provide the accuracy of each model individually.

There are also privacy methods which are commonly used in practice but have not been studied in the forecasting literature. Top- and bottom-coding are used to replace the top (bottom) p percent of observations with the $1 - p$ (p) quantile. These methods are useful for protecting data with sensitive values in the tails of distributions, such as income levels or smart meter data. (Crimi & Eddy, 2014) study the effect of top coding the Census' Public Use Microdata Samples on analyses of interest. They find that the sample correlation between two variables is shrunk towards zero when one or both of the variables are top coded. This may be relevant to multivariate forecasting model accuracy, which relies on the correlations between time series, and may be negatively affected when series are top- or bottom-coded. On the other hand, top- and bottom-coding could have an effect similar to adjusting for outliers, which can improve forecast accuracy when the outliers are close to the forecast origin (Chen & Liu, 1993).

Overall, while recent attention has been paid to privacy preserving collaborative forecasting, our interest is in forecasting using a single protected dataset. There has been no work which compares multiple forecasting models' accuracies when forecasting for a single protected dataset, or a comparison of models' accuracies under various privacy methods. The works which have shown

that data protection degrades forecast accuracy have also not given detailed explanations as to why model performance is worse on protected data. Finally, there exist no privacy methods which are specifically designed with forecasters in mind, which our work remedies.

2.1. Privacy Adjusted Forecasts

Judgmental adjustments to forecasts can improve accuracy by accounting for information that was not incorporated into a forecasting model (Fildes et al., 2009). Incorporating the intuition and experience of the adjuster, knowledge of special events, or insider or confidential information can add information with high diagnosticity that is useful for forecasting. However, adding information with low diagnosticity can degrade forecast accuracy (Fildes et al., 2019). Adjusting forecasts for the sake of gaining control of the forecasting process, incorporating practitioner expectations, and compensating for judgmental biases can be detrimental to forecast accuracy ((Petropoulos et al., 2022) section 3.7.3). Despite varying motivations for judgmentally adjusting forecasts, these adjustments have been found to improve the accuracy of monthly demand forecasts from statistical models by an average of 10% (Davydenko & Fildes, 2013). The accuracy improvements are greater for low volatility time series which are easier to forecast (Fildes et al., 2009).

The characteristics of adjustments have an effect on forecast accuracy. Both positive and negative adjustments can improve accuracy, but positive adjustments tend to give only a marginal improvement (Davydenko & Fildes, 2013). Forecast bias can be reduced by negative adjustments, whereas positive adjustments maintain bias or exacerbate it (Fildes et al., 2009). The magnitude of judgmental adjustments is positively associated with the size of accuracy improvements, which can occur when larger adjustments are made by adjusters who are confident in reliable information (Fildes et al., 2009).

Regardless of the motivation for data protection, privacy methods alter time series features which leads models to generate different forecasts than what would be produced based on the original data. The 'adjustment' is applied to the data rather than directly to the forecasts, but both privacy protection and judgmental adjustments result in adjusted forecasts. However, privacy protection may be applied without regard for forecast accuracy. Privacy methods based on random noise add information with low diagnosticity, and are likely to reduce forecast accuracy. While the direction and size of adjustment are purposefully chosen in judgmental forecasting, the direction and size of adjustments to forecasts from privacy protection will be determined by forecasting models' response to changes in time series features. These responses are likely related to the strength of data protection changes in time series features. These responses are likely related to the strength of data protection since stronger data protection results in larger changes to the data.

2.2. Time Series Features and Forecasting

There are thousands of features which have been used for time series classification (Fulcher & There are thousands of features which have been used for time series classification (Fulcher & Jones, 2014). A smaller set of interpretable features was used by (Bandara et al., 2018) for clustering and forecasting similar time series, which improved the accuracy of recurrent neural network models. Our focus is on features which are predictive of forecast accuracy, since privacy methods which alter these features will be most detrimental for forecasting.

The initial results from the M4 competition suggested that the randomness and linearity of time series were the most important determinants of forecast accuracy, and that seasonal time series (which are typically less noisy) are easier to forecast (Makridakis et al., 2018). In a follow-up study, (Spiliotis et al., 2020) used multiple linear regression to confirm the importance of randomness, linearity, and seasonal strength in predicting the MASE values of the ETS, ARIMA, Theta, and Naïve 2 (random walk applied to seasonally adjusted data) models from the M4 competition. On average, increasing the frequency, kurtosis, linearity, and seasonal strength of time series contributed to improved forecast accuracy. However, increasing skewness, self-similarity, and randomness affected accuracy negatively. While strength of seasonality improved the accuracy of all models, strength of trend had no statistically significant effect on accuracy for ETS, ARIMA, and Theta, while hurting accuracy for Naïve 2, which has no means of accounting for trend.

Outside of predicting forecast accuracy, time series characteristics can be used as a basis for making and combining forecasts. Features such as the strength of trend and seasonality have been used in exponential smoothing model selection (Qi et al., 2022). Forecasts based on this feature-based model selection had lower MASE, sMAPE, and MSIS than information-based selection methods for the majority of forecast horizons. Time series characteristics have also been used to select optimal model and forecast combinations (Li et al., 2022; Talagala et al., 2022). Model selection based on the representativeness of forecasts (Petropoulos & Siemsen, 2022) selects models with trend and seasonality components when the respective signals of these components are strong, and has been shown to outperform information criteria-based and cross-validation based model selection.

2.3. Our Contributions

Our contributions are two-fold. First, we analyze privacy adjusted forecasts from multiple forecasting models and privacy methods. We extract time series features which are predictive of forecast accuracy and show how these features change under data protection. We use these changes to explain the performance of various forecasting models and provide recommendations on forecasting with protected data.

Second, we propose a novel privacy method designed with forecasters in mind. Existing privacy methods apply protection based on the values of time series and give no regard to the preservation of time series features. Due to the relationship between time series features and forecast accuracy, and the usefulness of time series features for performing model selection and forecast combination, existing privacy methods fail to provide utility for forecasting at meaningful levels of privacy. We address this issue using a matrix-based method which swaps the values of time series with We address this issue using a matrix-based method which swaps the values of time series with similar features to help maintain forecast accuracy. Results show that our method provides significantly better accuracy at similar levels of privacy protection compared to competitor privacy methods. We define our proposed method in the next section.

Commented [B2]: citations

Commented [B3R2]: "... we create a privacy method that uses a feedback loop based on time series features to forecast well under data protection."

Commented [B4R2]: Need strong case that features must be considered in data protection.

Commented [B5R2]: If you're just trying to preserve correlations, you can do differentially private correlations. You can't just consider a single feature though, you need multiple features which feed into the quality of forecasts.

3. The k-nearest Time Series (nTS) Swapping Method

See attached pdf.

4. Time Series Features for Swapping Protection

In this section, we describe the time series features which have been demonstrated to have a relationship with forecast accuracy. We let x_j' denote a univariate stationary time series with a finite mean and constant variance. The spectral density $f_x(\lambda)$ of x_j' is estimated as the scaled fourier transform of the autocovariance function $\gamma_x(k)$ of x_j'. The spectral density can be thought of as the probability density function of a random variable Λ on the unit circle (Goerg, n.d.), where for a non-zero integer k, when $\gamma_x(k) \neq 0$, the spectral density $f_x(\lambda)$ will have a peak at the corresponding frequency λ. The forecastability, or spectral entropy, of x_j' is measured using the Shannon entropy of $f_x(\lambda)$, given by

$$SpecEntropy = -\int_{-\pi}^{\pi} \widehat{f_x}(\lambda) log\, \widehat{f_x}(\lambda) d$$

where the maximum entropy is attained when $\Lambda \sim U(-\pi, \pi)$. In practice, estimates of $F_1 \in [0,1]$, where high F_1 values represent a low signal-to-noise ratio, indicating that x_j' is difficult to forecast (Kang et al., 2017).

Next, we consider the self-similarity feature quantified using the Hurst parameter (Wang et al., 2006), which measures the long-range dependence of a time series. This feature had the largest magnitude effect on forecast accuracy in the study of the M4 data performed by (Spiliotis et al. 2020). We use the definition of self-similarity of a time series described by (Willinger et al., n.d.). Suppose that x_j' is the increment process of x_j, i.e., $x_{j,t}' = x_{j,t+1} - x_{j,t}$

An aggregated sequence, denoted $x_j'^{(m)}$, is created by averaging x_j' over non-overlapping blocks of size m, where

$$x_{j,k}'^{(m)} = 1/m \sum_{i=(k-1)m+1}^{km} x_{j,i}', \quad k = 1,2, \ldots$$

and k indexes the block. If x_j is a self-similar time series, then

$$x_j' = m^{1-H} x_j'^{(m)}$$

for all integers m. We focus on the definition of second-order self-similarity, where x_j' is exactly second-order self-similar if $m^{1-H} x_j'^{(m)}$ has the same variance and autocorrelation as x_j' for all values of m, or is asymptotically second-order self-similar if this holds as $m \to \infty$ (Rose, n.d.). The parameter H is the Hurst exponent, which is estimated using the differencing term d from a fractional ARIMA model, i.e., FARIMA(0, d, 0) (Wang et al., 2006) (Hyndman et al., 2022), where

$$Hurst = H = d + 0.5.$$

Estimates of H fall in the interval (0, 1), where $H = 0.5$ corresponds to a random walk (Sobolev, 2017), $H < 0.5$ corresponds to anti-persistent or mean-reverting series, and $H > 0.5$ corresponds to persistent time series that are more likely to maintain their current trend. (Rose, n.d.) notes that a self-similar process has a spectral density that follows a power law near $\lambda = 0$, where $f_x(\lambda) \sim a\lambda^{1-2H}$ as $\lambda \to 0$ with $0.5 < H < 1$. When $H \approx 1$, the spectral density increases rapidly as $\lambda \to 0$ and will tend to have low spectral entropy, whereas when $H \approx 0.5$, the spectral density

increases slowly as $\lambda \to 0$ and will tend to have high spectral entropy. For a random walk with $H = 0.5$, i.e., the spectral density is finite at the origin (Rose, n.d.).

We consider the remaining features from (Spiliotis et al., 2020) which had the largest effects on forecast accuracy. Since none of the privacy methods we consider will change the time series' frequency, we omit this feature from consideration, noting that higher frequencies are associated with improved forecast accuracy. We include skewness and kurtosis which measure the shape of the distribution of time series' values.

Skewness, which we denote F_3, measures the lack of symmetry in the distribution of the values of x_j (Wang et al., 2006), where positive (negative) values are associated with a right- (left-) skewed data distribution:

$$Skewness = \frac{1}{n\sigma^3}\sum_{t=1}^{n}\left(x_j - \bar{x_j}\right)^3$$

We use a measure of Kurtosis relative to the standard normal distribution (Wang et al., 2006). Positive kurtosis corresponds to distributions that tend to have a distinct peak near the mean with heavy tails, whereas negative kurtosis corresponds to distributions that are relatively flat near the mean,

$$Kurtosis = \frac{1}{n\sigma^4}\sum_{t=1}^{n}\left(x_j - \bar{x_j}\right)^4 - 3,$$

where 3 is the kurtosis of the standard normal distribution.

Next, we perform STL decomposition (Cleveland et al. 1990) to obtain the trend, seasonal, and remainder components of x_j. We use the approach of (Hyndman et al. 2019) which is designed to handle multiple seasonalities to obtain

$$x_j = f_j + s_{1,j} + \cdots + s_{M,j} + e_t,$$

where f_j, $s_{i,j}$, and e_j are the trend, ith Seasonal, and remainder components, respectively.

We extract the first order autocorrelation coefficient of the detrended and deseasonalized series, referred to as 'linearity' by (Spiliotis et al. 2018).

$$E\_acf = \frac{\sum_{t=2}^{T}(e_{j,t}-\bar{e})(e_{j,t-1}-\bar{e})}{\sum_{t=1}^{T}\left(e_{j,t}-\bar{e}\right)^2}$$

This feature gives a measure of the forecastability of a time series after the trend and seasonality have been accounted for.

Continuing with the decomposed series, we compute the strength of trend F_6 and strength of the ith seasonal component $F_{7,i}$ as follows,

$$Trend = 1 - \frac{Var(e_j)}{Var(f_j + e_j)},$$

$$Seasonality_i = 1 - \frac{Var(e_j)}{Var(s_{i,j} + e_j)}.$$

In practice, the values of $Trend$ and $Seasonality_i$ are bounded to [0,1] (Hyndman 2022).

Our final two features are included to maintain data utility throughout the k-nTS swapping process. The idea is to swap values between series that not only have similar characteristics, but whose values have similar magnitudes. Toward this end, we include the mean F_8 and the variance F_9 of x_j,

$$SeriesMean = \frac{1}{T}\sum_{t=1}^{T} x_{j,t},$$

$$SeriesVariance = \frac{1}{T-1}\sum_{t=1}^{T}\left(x_{j,t} - \bar{x}_j\right)^2.$$

Figure 3 compares two monthly time series on the nine time series features discussed in this section. The good forecastability of the series on the left is indicated by the low spectral entropy and high Hurst coefficient values. The series on the right, however, is essentially a random walk as indicated by the value of the Hurst coefficient, and a spectral entropy of one indicates a very low signal to noise ratio. Another notable difference is in the strength of the trend of each series – most of the variance of the series on the left is due to a strong trend, which is forecastable, whereas the variance in the series on the right appears to be due to the randomness of the series. The series on the left has low *Kurtosis*, i.e., light tails relative to the standard normal distribution, whereas the opposite is true for the series on the right.

Fig 3: Comparison of a time series with desirable features (easy to forecast) and a time series with undesirable features (difficult to forecast).

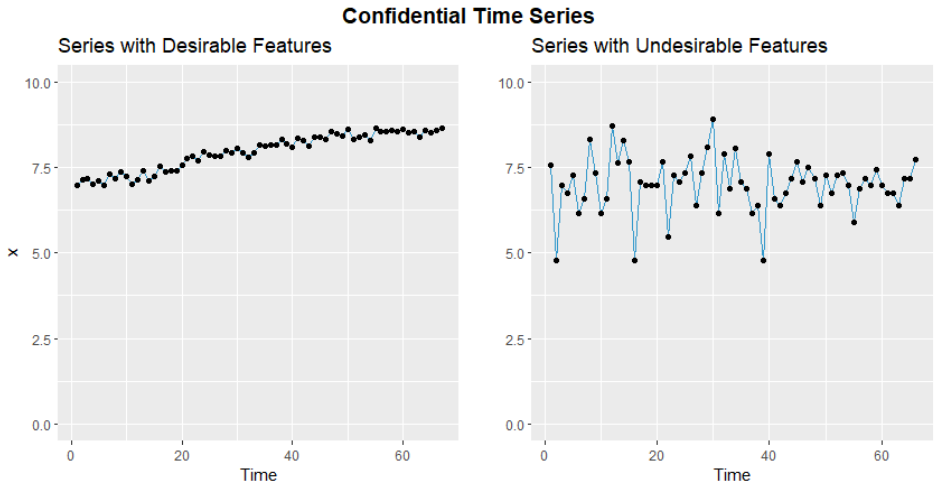

Table 2: feature value comparison between a series with desirable features (easy to forecast) and a series with undesirable features (difficult to forecast)

Feature	Desirable Features (left Fig. 1)	Undesirable Features (right Fig. 1)
SpecEntropy	0.07	1.00
Hurst	1.00	0.50
Skewness	-0.42	-0.57
Kurtosis	-1.24	1.16
E_acf	-0.09	-0.19
Trend	0.97	0.12
Seasonality	0.16	0.23
SeriesMean	7.96	7.01
SeriesVariance	0.29	0.65

5. The *k*-nearest Time Series + (nTS+) Swapping Method

The *k*-nTS+ privacy method builds on *k*-nTS by including a feature selection process based on the changes in time series features and forecast accuracy under baseline privacy methods. The idea is to perform swapping which limits the changes in features which are most predictive of changes in forecast accuracy.

The feature selection process starts with the data controller generating forecasts for period $T - 1$ for both the original data and the data protected using baseline privacy methods such as differential privacy and additive noise. The data controller measures the *difference* in forecast errors, denoted e_j^d, and time series feature values, denoted f_j^d for feature f, between each original and protected time series. Our reasoning is that a feature should be included in the *k*-nTS swapping process if changes in that feature are predictive of changes in forecast error.

We perform a two-stage feature selection process. An initial filtering of the features is performed by the RReliefF algorithm (Robnik-Sikonja & Kononenko 2003) which assigns a weight to each feature that indicates the ability of changes in that feature to predict changes in forecast accuracy. Next, we use random forest to generate permutation-based feature importance scores for the features with the largest RReliefF weights. Ultimately, we include the subset of features that have the largest importance values based on the random forest.

The *k*-nTS+ algorithm can be used collaboratively between the data controller and the forecaster. If, for example, the forecaster specifies their preferred forecasting model(s), the data controller can apply the model(s) to the original and protected data up through time period $T - 1$, assess which changes in features are most predictive of changes in accuracy for the specified model(s), and release data to the forecaster using *k*-nTS+ based on these features up through time period T.

~~**The *k*-nearest Time Series (nTS) Swapping Method**~~

6. Empirical Application

6.1. Data

Recent work by (Spiliotis et al., 2020) showed that the M3 competition data are representative of the real world on the basis of time series characteristics. Complex forecasting models are known to forecast more accurately than simple models using the unprotected version of the M3 competition monthly micro data (Koning et al., 2005), and models that explicitly capture trend and seasonality performed the best in the overall M3 competition (Makridakis & Hibon, 2000). We are interested in whether these results hold when forecasting using protected versions of the data. For our analyses, we use the monthly micro dataset from the M3 competition, which includes 474 strictly positive time series with values ranging from 120 to 18,100. Of the 474 series, 18 consist of 67 time periods, 259 consist of 68 time periods, and 197 consist of 125 time periods.

Commented [B7]: Need to be convincing that this data set must be used.

Commented [B8R7]: Requirements:
(1) representative of time series features
(2) Complex methods need to forecast better
(3) Replicability - enables testing of other privacy methods.
(4) research on the features (Spiliotis et al. 2020)

6.2. Forecasting Models

The forecasting models under study are separated into "simple" models which are trained to forecast one series at a time, and "complex" models which are trained to generate forecasts for multiple series. We perform minimal data pre-processing and allow the models to capture the important components of the series. Our goal is to assess the effects of privacy protection on the accuracy of popular forecasting models which are readily available to implement in R and/or Python and have served as benchmarks or winners in recent forecasting competitions. Additional model descriptions are given in Section 5.4, where we explore the performance of each model mathematically based on the time series features. Please see the appendix for full implementation details.

Table 3: forecasting models under study. Includes relevant information for the variant of model and whether it is a local or global forecasting model. We consider the VAR somewhere in between a local and a global model – it must be trained on subsets of the M3 data due to its computational complexity.

	Model Name	Variant	Global (Yes/No)
Simple Models	SES	-	N
	DES	Additive trend	N
	TES	Additive trend/seasonality	N
	Auto-ARIMA	seasonal	N
Complex Models	VAR	-	-
	LGBM	-	Y
	RNN	LSTM	Y

6.3. ~~Competitor~~ Privacy Methods

Formatted: Outline numbered + Level: 2 + Numbering Style: 1, 2, 3, … + Start at: 1 + Alignment: Left + Aligned at: 0.25" + Indent at: 0.55"

We apply each of the privacy methods shown in Table 3 below to the original M3 monthly micro data for each of the displayed parameter values.

Table 3: privacy methods, and their parameter values, which we apply to the m3 monthly micro data. Values are arranged in order of strength of privacy protection.

Privacy Method	*Parameter*	*Values*
Additive Noise	s	0.25, 0.50, 1.0, 1.5, 2.0
Differential Privacy	ϵ	20.0, 10.0, 4.6, 1.0, 0.1
k-nTS	k	3, 5, 7, 10, 15
k-nTS+	k	3, 5, 7, 10, 15

~~6.2.~~6.3.1. *Differential Privacy*

Given an original ~~confidential~~ time series $\boldsymbol{A}$, a differentially private time series can be created using a randomized mechanism $M(\mathbf{A}) = \mathbf{A} + \mathbf{N}$ which adds Laplace random noise $\boldsymbol{N}$ with scale parameter $\Delta f_1/\epsilon$. The sensitivity Δf_1 is determined as the maximum absolute difference between two time series $\boldsymbol{A}$ and $\boldsymbol{A}'$, which differ in at most one observation, where $\Delta f_1 = max||A - A'||_1$. The mechanism M satisfies ϵ-differential privacy by guaranteeing that, for every output $\boldsymbol{t}$ of M and every pair of series $\boldsymbol{A}$ and $\boldsymbol{A}'$,

$$Pr(M(\boldsymbol{A}) = \boldsymbol{t}) \leq exp(\epsilon) Pr(M(\boldsymbol{A}') = \boldsymbol{t}).$$

6.3.2. *Additive Noise*

Additive noise protection is achieved by adding a normal random number with mean zero and standard deviation σ to each ~~confidential v~~value in a time series x_j. Protected values can be written $P_{j,t} = A_{j,t} + r$, where $r \sim N(0, \sigma^2)$ and $\sigma = s * \sqrt{\left(E\left[\left(x_j - E[x_j]\right)^2\right]\right)}$. The protection parameter s denotes the number of standard deviations of x_j that define the standard deviation of the sampling distribution of r.

~~*k-nTS+ Feature Selection*~~

6.3.3. *k-nTS and k-nTS+*

For *k*-nTS, the distance between time series is calculated using the nine features described in Section 4.3.

To perform feature selection for *k*-nTS+, we create protected versions of our selected data using additive noise and differential privacy for all of the parameter values shown in Table 3 (i.e., 10 protected data sets and 1 original data set). We generate forecasts for each of the 11 data sets for time period $T - 1$ using each of the forecasting models shown in Table 3 and compute the absolute error of each forecast for each series. We compute the differences in the absolute error between the original and protected forecasts for each series and model and use these differences as the target variable in the RReliefF algorithm. Next, we compute 39 time series features using the tsfeatures package in R, including the nine features described in Section 3. Using RReliefF, the differences in these features for each series are used to predict the differences in absolute forecast~~ting~~ errors for each series between the original and protected data sets. Figure 4 shows the RReliefF weights for each of the 39 features.

Figure 4: Feature weights from RReliefF algorithm.

Formatted: Font: Cambria, Italic

Formatted: Normal, No bullets or numbering

Formatted: Indent: Left: 0.55", No bullets or numbering

Formatted: Font: Cambria, Italic

Formatted

Commented [B9]: Could say we do not consider top/bottom coding because it can be accounted for (censored model)

Formatted: Outline numbered + Level: 3 + Numbering Style: 1, 2, 3, … + Start at: 1 + Alignment: Left + Aligned at: 0.5" + Indent at: 0.85"

Formatted: Font: Italic

Formatted: List Paragraph, Indent: Left: 0.85"

Formatted: Font: (Default) Cambria, Italic

Formatted: List Paragraph, Outline numbered + Level: 3 + Numbering Style: 1, 2, 3, … + Start at: 1 + Alignment: Left + Aligned at: 0.5" + Indent at: 0.85"

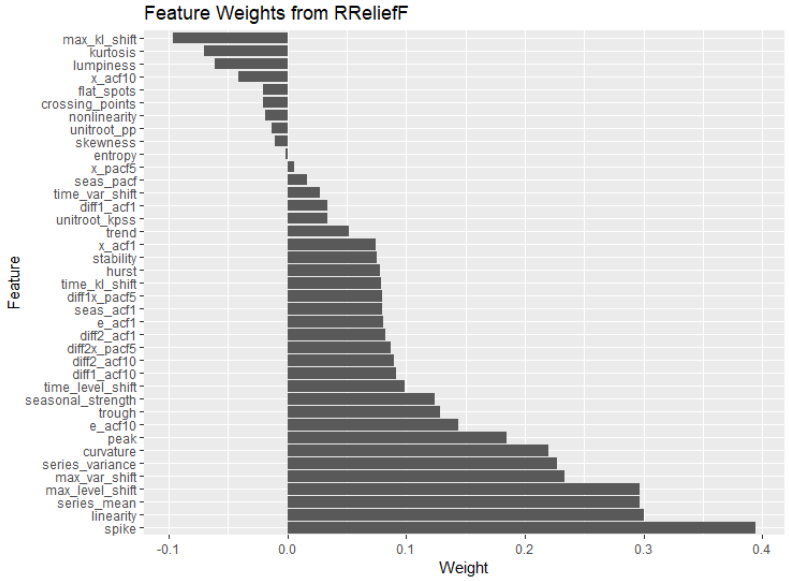

Severa weights. Many atures with weights greater than 0.10 for inclusion in the random forest. We include all features with RReliefF weights greater than 0.10 in the random forest selection procedure, and those results are shown in Figure 5. The random forest flags several features as poor predictors of changes in forecast error, assigned them negative weights. We include the features with positive random forest importance values in *k*-nTS+. These features and their descriptions are shown in Table 4.

FIG 5: Random forest feature importance results.

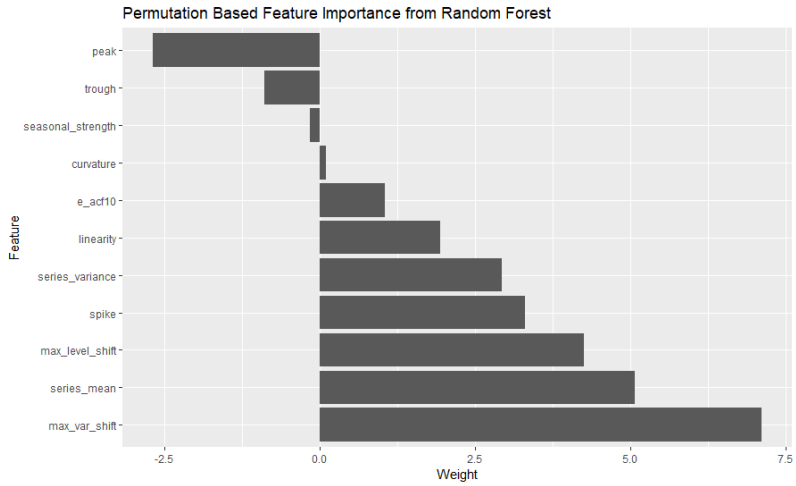

Table 4: Names and descriptions of features selected for *k*-nTS+.

Feature Type	Feature Name	Description
Overall Shape/Location	series_mean	Mean of the time series.
	series_variance ~~max_var_shift~~	Variance of the time series.~~Largest shift in the variance between two consecutive sliding windows.~~
	linearity ~~series_mean~~	First non-intercept coefficient of an orthogonal quadratic regression.~~Mean of the time series.~~
	curvature ~~max_level_shift~~	Second non-intercept coefficient of an orthogonal quadratic regression.~~Largest shift between the means of two consecutive sliding windows.~~
Changes in Shape/Location	max_var_shift ~~spike~~	Largest shift in the variance between two consecutive sliding windows.~~Variance of the leave-one-out variances of the remainder component of the decomposed series.~~
	max_level_shift ~~series_variance~~	Largest shift between the means of two consecutive sliding windows.~~Variance of the time series.~~
Remainder Component Characteristics	spike	Variance of the leave-one-out variances of the remainder component of the decomposed series.
	e_acf10	Sum of the first ten squared autocorrelation coefficients of the remainder component of the series.

The features selected for *k*-nTS+ can be divided into three groups. The first group, consisting of the mean, variance, linearity, and curvature, defines the overall shape of a time series (in this case the overall shape of the series within the sliding window). The second group measures shifts in the location (mean) and shape (variance) within a time series window. The third group captures important characteristics of the remainder component.

Figure X compares some protected versions of the series with desirable and undesirable features from Section 4.

Figure X: Comparison of original, AN (s = 1), and *k*-nTS+ (*k* = 7) versions of the series with desirable and undesirable features.

Formatted Table
Formatted: Not Highlight
Formatted: Not Highlight
Formatted: Not Highlight
Formatted: Not Highlight
Formatted: Not Highlight
Formatted: Not Highlight
Formatted: Not Highlight

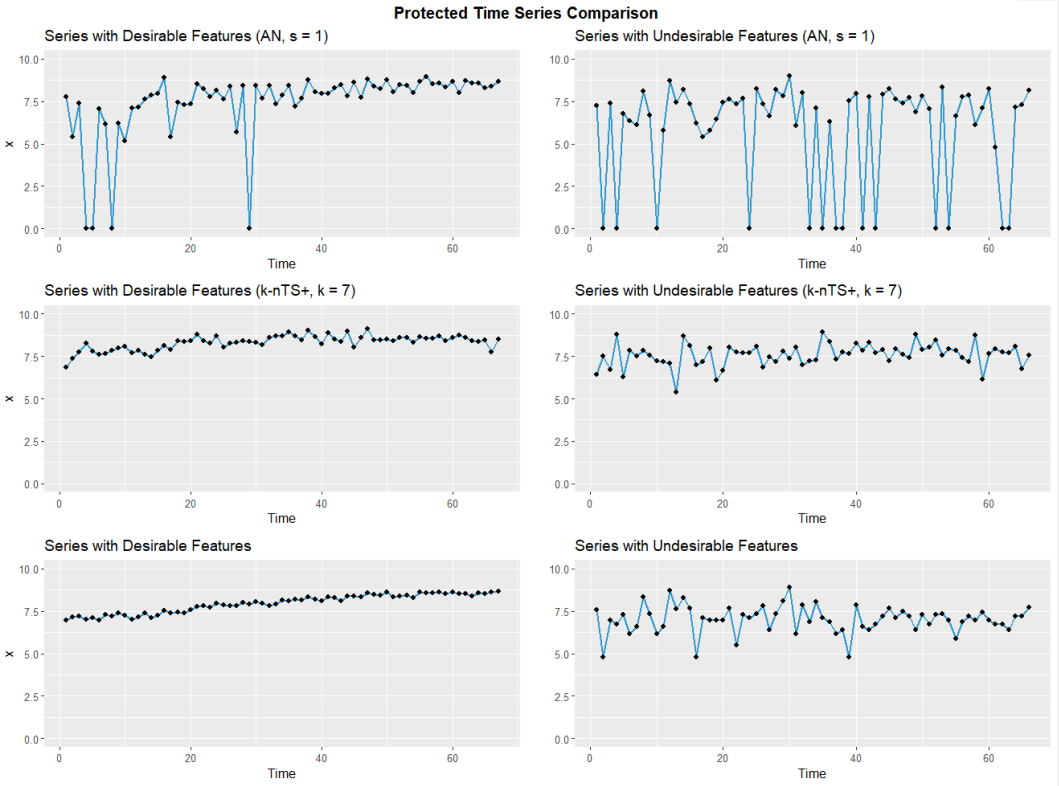

6.4. Forecast Accuracy and Privacy Assessment

We assess the ability of each privacy method to protect against *identification disclosure*, which occurs when a third party correctly predicts the identity of a protected time series.

For brevity, we have included the math behind our definition of identification disclosure in the appendix. The metric we use to measure the risk of identification disclosure, $\bar{P}$, gives the average proportion of the J time series which are correctly identified across S simulated privacy attacks:

$$\bar{P} = \frac{1}{J * S} \sum_{s=1}^{S} \sum_{i=1}^{J} [\widehat{M_i^s} = j^*]$$

where $\widehat{M_i^s}$ is the third party's prediction of the identity of the ith protected time series, and identification disclosure occurs when the predicted identity is equal to the true identity j^*.

Table 5 contains the average MAE of one-step ahead point forecasts across all models, and the identification disclosure metric $\bar{P}$, for several privacy parameters for each privacy method. For the simulated privacy attacks, we extract $S = 20$ random samples of external data containing ten values from each time series. There is a clear relationship between forecast accuracy and the strength of privacy protection. While strong differential privacy provides the lowest risk of identification and attribute disclosure, it more than triples the average forecast error relative to the original data. Essentially unusable forecasts are produced under differential privacy and additive noise unless privacy is quite weak ($\epsilon = 10$, or $s = 1$). For example, under differential privacy with $\epsilon = 10$, nearly 50% of series are identified correctly on average, while MAE has increased by just over 30%. Protection against identification disclosure is better under additive noise with $s = 1$: about 22% of series are correctly identified on average. But, this comes at further cost to forecast accuracy, which is reduced by nearly 45%. Standard k-nTS with $k = 3$ offers a better trade-off – protection against identification disclosure is quite good, since only 2% of series are correctly identified on average, while accuracy is reduced by about 40%. So, for a similar reduction in accuracy to additive noise with $s = 1$, k-nTS gives better privacy. k-nTS+ offers better protection against identification disclosure than additive noise ($s = 1$) and differential privacy ($\epsilon = 10$) with a reduction in accuracy of only 13%.

		Privacy Method											
	Original	Additive Noise			Differential Privacy			*k*-nTS			*k*-nTS+		
Parameter	-	1.0	1.5	2.0	10	4.6	1.0	3	7	15	3	7	15
AvgPropIdent	-	22.29	9.99%	5.57	48.66	12.44	1.95	2.03	2.00	1.96	4.5	3.58	3.28
Average MAE	685.71	993.95	1343.29	1821.38	899.38	1400.95	3310.34	956.89	987.04	1066.16	778.27	797.91	848.11

Commented [B11]: Make sure epsilon value for DP is correct - review write-up on it. Make sure it is still differentially private in the presence of external information.

Commented [B10]: Include representativeness in table?

* The average across models for additive noise and differential privacy excludes the VAR model error for AN (s = 1) and DP ($\epsilon = 0.1$) as the errors in these cases were over 1000% larger than the error of any other model. The reasons for this will be explored in section -.

In **Table 4,** the models are rank-ordered based on their MAE on the original data. We also display the rank of each model based on forecast error variance. TES and ARIMA, which explicitly model the seasonality of the series, had the best accuracy which is consistent with the findings of the original M3 competition (Makridakis & Hibon, 2000). These models also had the lowest error variance. However, their performance suffers on the protected data, as the SES, DES, and RNN models outperform them on both accuracy and error variance. Overall, DES and SES are the simplest models and have the best accuracy and lowest error variance across protected data sets. LGBM is ranked equal to Auto-ARIMA on average rank, while VAR consistently performs the worst.

Table 4: the rank of each model in terms of MAE and forecast error variance on the original data vs. the average rank across protected datasets. The rightmost column contains the average of the protected MAE and error variance ranks.

	MAE Ranks		Forecast Error Variance Ranks		Average Rank
Model	Original	Protected	Original	Protected	Protected
TES	1	4.5	2	3.5	4
ARIMA	2	4.5	1	4.25	4.38
RNN	3	3	5	3.25	3.13
DES	4	2.5	3	2	2.25
SES	5	2.5	4	3.25	2.88
LGBM	6	4	7	4.75	4.38
VAR	7	7.0	6	7	7

~~To perform identification disclosure, we assume a third party possesses some confidential data pertaining to a unit of interest in the protected dataset. For the above example, this would be some sequence of confidential daily sales quantities for a known retailer. Denote this confidential data $c_t = (ID_t, c_t)$, which contains a direct identifier ID_t (e.g., the identity of retailer i) and confidential data $c_t = (A_{t,t^*}, \dots, A_{t,t^*+L})$ which contains a sequence of confidential values which are components of the confidential time series x_j.~~

~~We let M_t denote the random variable (from the perspective of the third party) that indicates the corresponding PID_j for ID_t, i.e., $M_t = j$ when the confidential values in c_t are components of the confidential version of protected series j. Since the true value $M_t = j^*$ is unknown, the third party predicts the value of M_t to be the series j with the highest match probability, conditional on the known confidential values, as follows~~

$$\widehat{M}_t = argmax_j P(M_t = j|c_t), \quad (1)$$

~~where identification disclosure occurs when $\widehat{M}_t = j^*$. The probability $P(M_t = j|c_t)$ is calculated as follows. Let $\tilde{x}_j = (P_{j,t^*}, \dots, P_{j,t^*+L}), j = 1, \dots, J$ denote the protected values of each time series j that occur in the same time periods as c_t. The third party computes the similarity between c_t and the protected values $\tilde{x}_j, j = 1, \dots, J$ using the Euclidean distance,~~

$$s(c_t, \tilde{x}_j) = \frac{1}{||c_t - \tilde{x}_j||_2}, j = 1, \dots, J.$$

6.5. Changes in Time Series Features

In **Figure 5**, we calculate the average feature value for each series across the protected datasets for each privacy method. We plot these distributions next to the distribution of each feature from the original data.

Commented [B16]: Polar coordinate plots for time series

Figure 5: distributions of the original feature values for each series and the average feature values for each series across protected datasets for each privacy method.

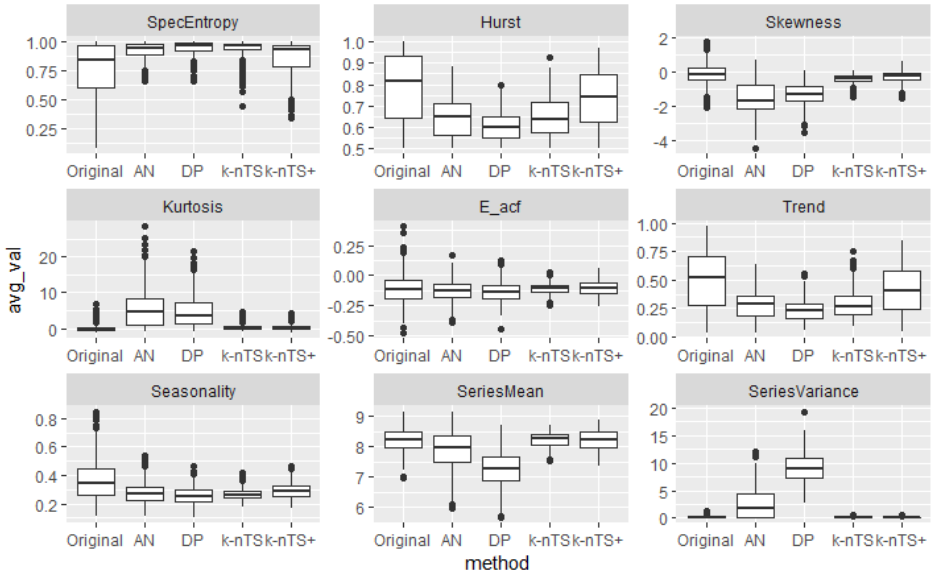

- While all privacy methods tend to increase spectral entropy, the distribution under *k*-nTS+ is much closer to the original than the other methods.
- The most notable differences between the privacy methods show up in skewness, kurtosis, series mean, and series variance.
    - Random noise-based protection produces a negative skew in log-transformed time series, creates heavy tails, biases the mean downward, and blows up the variance.

Standard

K-nTS increases the randomness and reduces the long-term dependence of series,

- Distributional features, namely *SeriesVariance*, *SeriesMean*, *Skewness*, and *Kurtosis*, are much less affected under standard k-nTS than random noise protection.
- The features selected in *k*-nTS+ are the "building blocks" for maintaining the other features such as Hurst coefficient and the strength of trend.
- None of the protection methods appear to do particularly well at preserving the strength of seasonality, although features related to seasonality (strength of seasonality,

peak, and trough) were determined not to be useful for predicting changes in forecast error from data protection (for this particular data set).

- Overall, k-nTS makes the series more random, but preserves some of their distributional patterns. K-nTS+ does a better job of preserving the spectral entropy, hurst, and strength of trend, leading to improved forecast accuracy.
- Random noise protection produces large changes both in the distributions of time series increases their randomness, and poor forecast accuracy.

Commented [B17]: Representativeness comparison to originals - if series are representative, it could increase trust in protected data and willingness to protect

Commented [B18R17]: If a protected forecast is representative of the original data, is that is a good thing?

1.1.6.6. *Detailed Model Performance Explanations*

Commented [B23]: Matter of fact section on how features change model equations - invariant to data set.

The simplest model we examine is SES, where the forecast for time period $t + h$ is a weighted average of the time series values up through time period t.

$$\hat{x}_{t+h|t} = l_t$$
$$l_t = \alpha x_t + (1-\alpha) l_{t-1}.$$

Changes in the distribution of x_t will directly affect the value of the level l_t. For example, positively (negatively) skewing the distribution of x_t will shift the level in the positive (negative) direction, directly affecting the accuracy of the forecasts.

In terms of model fitting, SES tends to select smaller values of α when applied to data that is less forecastable. Figure 5 shows that on average, the value of α is lower for series with higher spectral entropies and lower Hurst coefficients. The good news is that this means SES is not treating the random noise in the series as a signal, and instead tends to smooth it out.

Fig 5: Average SES α value and level l_t across series and protected data sets for each privacy method.

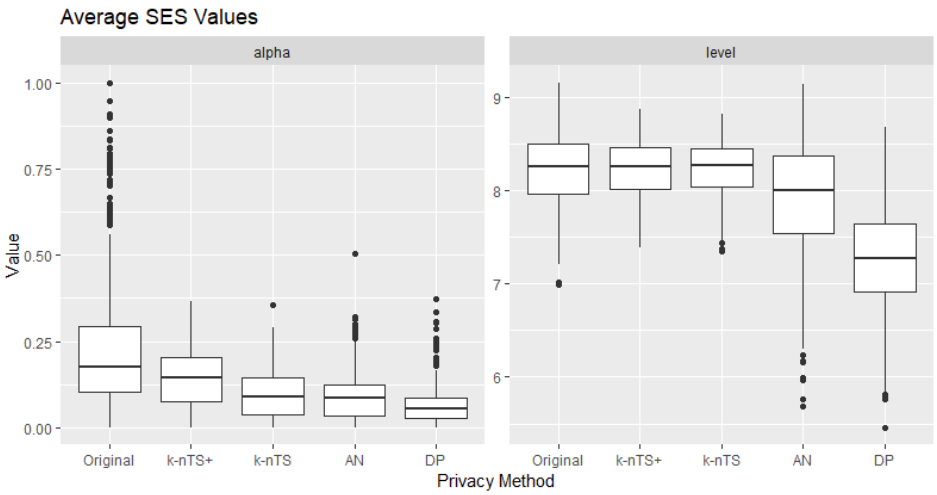

DES builds on SES by accounting for the trend of a series,

$$\hat{x}_{t+h|t} = l_t + hb_t$$
$$l_t = \alpha x_t + (1-\alpha)(l_{t-1} + b_{t-1})$$
$$b_t = \beta(l_t - l_{t-1}) + (1-\beta)b_{t-1}.$$

TES builds on DES by incorporating seasonal components,

$$\hat{x}_{t+h|t} = l_t + hb_t + s_{t+h-m(k+1)}$$
$$l_t = \alpha(x_t - s_{t-m}) + (1-\alpha)(l_{t-1} + b_{t-1})$$
$$b_t = \beta(l_t - l_{t-1}) + (1-\beta)b_{t-1}$$
$$s_t = \gamma(y_t - l_{t-1} - b_{t-1}) + (1-\gamma)s_{t-m}.$$

The ARIMA$(p,d,q)(P,D,Q)_m$ model is a function of p autoregressive parameters ϕ_p, P seasonal autoregressive parameters Φ_P, q moving average parameters θ_q, and Q seasonal moving average parameters Θ_Q.

$$x_t = c + \phi_1 x_{t-1} + \cdots + \phi_p x_{t-p} +$$
$$\theta_1 \epsilon_{t-1} + \cdots + \theta_q \epsilon_{t-q} +$$
$$\Phi_1 x_{t-m} + \cdots + \Phi_P x_{t-mP} +$$
$$\Theta_1 \epsilon_{t-m} + \Theta_Q \epsilon_{t-mQ} + \epsilon_t.$$

The VAR model forecasts K time series where the forecast for series k is a function of p lagged values of series k and each of the other $k-1$ series,

$$x_{k,t} = c_k + \phi_{k1,1} x_{1,t-1} + \phi_{k2,1} x_{2,t-1} + \cdots + \phi_{kk,1} x_{k,t-1} +$$
$$\phi_{k1,2} x_{1,t-2} + \cdots + \phi_{kk,p} x_{k,t-p} + \epsilon_{k,t}$$

7. Conclusions

References

Abowd, J. M., Gittings, K., McKinney, K. L., Stephens, B. E., Vilhuber, L., & Woodcock, S. (2012). *Dynamically consistent noise infusion and partially synthetic data as confidentiality protection measures for related time-series*. 41.

Bandara, K., Bergmeir, C., & Smyl, S. (2018). Forecasting Across Time Series Databases using Recurrent Neural Networks on Groups of Similar Series: A Clustering Approach. *ArXiv:1710.03222 [Cs, Econ, Stat]*. http://arxiv.org/abs/1710.03222

Boone, T., Ganeshan, R., Jain, A., & Sanders, N. R. (2019). Forecasting sales in the supply chain: Consumer analytics in the big data era. *International Journal of Forecasting*, *35*(1), 170–180. https://doi.org/10.1016/j.ijforecast.2018.09.003

Chen, C., & Liu, L.-M. (1993). Forecasting time series with outliers. *Journal of Forecasting*, *12*(1), 13–35. https://doi.org/10.1002/for.3980120103

Crimi, N., & Eddy, W. (2014). Top-Coding and Public Use Microdata Samples from the U.S. Census Bureau. *Journal of Privacy and Confidentiality*, *6*(2). https://doi.org/10.29012/jpc.v6i2.639

Davydenko, A., & Fildes, R. (2013). Measuring forecasting accuracy: The case of judgmental adjustments to SKU-level demand forecasts. *International Journal of Forecasting*, *29*(3), 510–522. https://doi.org/10.1016/j.ijforecast.2012.09.002

de Montjoye, Y.-A., Hidalgo, C. A., Verleysen, M., & Blondel, V. D. (2013). Unique in the Crowd: The privacy bounds of human mobility. *Scientific Reports*, *3*(1), 1376. https://doi.org/10.1038/srep01376

Fildes, R., Goodwin, P., Lawrence, M., & Nikolopoulos, K. (2009). Effective forecasting and judgmental adjustments: An empirical evaluation and strategies for improvement in supply-chain planning. *International Journal of Forecasting*, *25*(1), 3–23. https://doi.org/10.1016/j.ijforecast.2008.11.010

Fildes, R., Goodwin, P., & Önkal, D. (2019). Use and misuse of information in supply chain forecasting of promotion effects. *International Journal of Forecasting*, *35*(1), 144–156. https://doi.org/10.1016/j.ijforecast.2017.12.006

Fulcher, B. D., & Jones, N. S. (2014). Highly Comparative Feature-Based Time-Series Classification. *IEEE Transactions on Knowledge and Data Engineering*, *26*(12), 3026–3037. https://doi.org/10.1109/TKDE.2014.2316504

Goerg, G. M. (n.d.). *Forecastable Component Analysis*. 9.

Goldfarb, A., & Tucker, C. (n.d.). *Why Managing Consumer Privacy Can Be an Opportunity*. 6.

Goldfarb, A., & Tucker, C. E. (2011). Privacy Regulation and Online Advertising. *Management Science*, *57*(1), 57–71. https://doi.org/10.1287/mnsc.1100.1246

Gonçalves, C., Bessa, R. J., & Pinson, P. (2021). A critical overview of privacy-preserving approaches for collaborative forecasting. *International Journal of Forecasting*, *37*(1), 322–342. https://doi.org/10.1016/j.ijforecast.2020.06.003

Goncalves, C., Bessa, R. J., & Pinson, P. (2021). Privacy-Preserving Distributed Learning for Renewable Energy Forecasting. *IEEE Transactions on Sustainable Energy*, *12*(3), 1777–1787. https://doi.org/10.1109/TSTE.2021.3065117

Goncalves, C., Pinson, P., & Bessa, R. J. (2021). Towards Data Markets in Renewable Energy Forecasting. *IEEE Transactions on Sustainable Energy*, *12*(1), 533–542. https://doi.org/10.1109/TSTE.2020.3009615

Hewamalage, H., Bergmeir, C., & Bandara, K. (2021). Recurrent Neural Networks for Time Series Forecasting: Current status and future directions. *International Journal of Forecasting*, *37*(1), 388–427. https://doi.org/10.1016/j.ijforecast.2020.06.008

Hewamalage, H., Bergmeir, C., & Bandara, K. (2022). Global models for time series forecasting: A Simulation study. *Pattern Recognition*, *124*, 108441. https://doi.org/10.1016/j.patcog.2021.108441

Imtiaz, S., Horchidan, S.-F., Abbas, Z., Arsalan, M., Chaudhry, H. N., & Vlassov, V. (2020). Privacy Preserving Time-Series Forecasting of User Health Data Streams. *2020 IEEE International Conference on Big Data (Big Data)*, 3428–3437. https://doi.org/10.1109/BigData50022.2020.9378186

Kang, Y., Hyndman, R. J., & Smith-Miles, K. (2017). Visualising forecasting algorithm performance using time series instance spaces. *International Journal of Forecasting*, *33*(2), 345–358. https://doi.org/10.1016/j.ijforecast.2016.09.004

Ke, G., Meng, Q., Finley, T., Wang, T., Chen, W., Ma, W., Ye, Q., & Liu, T.-Y. (n.d.). *LightGBM: A Highly Efficient Gradient Boosting Decision Tree*. 9.

Khosrowabadi, N., Hoberg, K., & Imdahl, C. (2022). Evaluating human behaviour in response to AI recommendations for judgemental forecasting. *European Journal of Operational Research*, *303*(3), 1151–1167. https://doi.org/10.1016/j.ejor.2022.03.017

Koning, A. J., Franses, P. H., Hibon, M., & Stekler, H. O. (2005). The M3 competition: Statistical tests of the results. *International Journal of Forecasting*, *21*(3), 397–409. https://doi.org/10.1016/j.ijforecast.2004.10.003

Li, L., Kang, Y., & Li, F. (2022). Bayesian forecast combination using time-varying features. *International Journal of Forecasting*, S0169207022000930. https://doi.org/10.1016/j.ijforecast.2022.06.002

Liyue Fan & Li Xiong. (2014). An Adaptive Approach to Real-Time Aggregate Monitoring With Differential Privacy. *IEEE Transactions on Knowledge and Data Engineering*, *26*(9), 2094–2106. https://doi.org/10.1109/TKDE.2013.96

Luo, J., Hong, T., & Fang, S.-C. (2018). Benchmarking robustness of load forecasting models under data integrity attacks. *International Journal of Forecasting*, *34*(1), 89–104. https://doi.org/10.1016/j.ijforecast.2017.08.004

Makridakis, S., & Hibon, M. (2000). The M3-Competition: Results, conclusions and implications. *International Journal of Forecasting*, *16*(4), 451–476. https://doi.org/10.1016/S0169-2070(00)00057-1

Makridakis, S., Spiliotis, E., & Assimakopoulos, V. (2018). The M4 Competition: Results, findings, conclusion and way forward. *International Journal of Forecasting*, *34*(4), 802–808. https://doi.org/10.1016/j.ijforecast.2018.06.001

Makridakis, S., Spiliotis, E., & Assimakopoulos, V. (2022). M5 accuracy competition: Results, findings, and conclusions. *International Journal of Forecasting*, S0169207021001874. https://doi.org/10.1016/j.ijforecast.2021.11.013

Martin, K. D., Borah, A., & Palmatier, R. W. (2017). Data Privacy: Effects on Customer and Firm Performance. *Journal of Marketing*, *81*(1), 36–58. https://doi.org/10.1509/jm.15.0497

Nicholson, W. B., Matteson, D. S., & Bien, J. (2017). VARX-L: Structured regularization for large vector autoregressions with exogenous variables. *International Journal of Forecasting*, *33*(3), 627–651. https://doi.org/10.1016/j.ijforecast.2017.01.003

Nin, J., & Torra, V. (2009). Towards the evaluation of time series protection methods. *Information Sciences*, *179*(11), 1663–1677. https://doi.org/10.1016/j.ins.2009.01.024

Petropoulos, F., Apiletti, D., Assimakopoulos, V., Babai, M. Z., Barrow, D. K., Taieb, S. B., Bergmeir, C., Bessa, R. J., Bijak, J., Boylan, J. E., Browell, J., Carnevale, C., Castle, J. L., Cirillo, P., Clements, M. P., Cordeiro, C., Oliveira, F. L. C., Baets, S. D., Dokumentov, A., … Ziel, F. (2022). *Forecasting: Theory and practice*. 167.

Petropoulos, F., & Siemsen, E. (2022). Forecast Selection and Representativeness. *Management Science*, mnsc.2022.4485. https://doi.org/10.1287/mnsc.2022.4485

Qi, L., Li, X., Wang, Q., & Jia, S. (2022). fETSmcs: Feature-based ETS model component selection. *International Journal of Forecasting*, S0169207022000954. https://doi.org/10.1016/j.ijforecast.2022.06.004

Smyl, S. (2020). A hybrid method of exponential smoothing and recurrent neural networks for time series forecasting. *International Journal of Forecasting*, *36*(1), 75–85. https://doi.org/10.1016/j.ijforecast.2019.03.017

Sobolev, D. (2017). The effect of price volatility on judgmental forecasts: The correlated response model. *International Journal of Forecasting*, *33*(3), 605–617. https://doi.org/10.1016/j.ijforecast.2017.01.009

Sommer, B., Pinson, P., Messner, J. W., & Obst, D. (2021). Online distributed learning in wind power forecasting. *International Journal of Forecasting*, *37*(1), 205–223. https://doi.org/10.1016/j.ijforecast.2020.04.004

Spiliotis, E., Kouloumos, A., Assimakopoulos, V., & Makridakis, S. (2020). Are forecasting competitions data representative of the reality? *International Journal of Forecasting*, *36*(1), 37–53. https://doi.org/10.1016/j.ijforecast.2018.12.007

Sweeney, L. (2002). k-ANONYMITY: A MODEL FOR PROTECTING PRIVACY. *International Journal of Uncertainty, Fuzziness and Knowledge-Based Systems*, *10*(05), 557–570. https://doi.org/10.1142/S0218488502001648

Talagala, T. S., Li, F., & Kang, Y. (2022). FFORMPP: Feature-based forecast model performance prediction. *International Journal of Forecasting*, *38*(3), 920–943. https://doi.org/10.1016/j.ijforecast.2021.07.002

Véliz, C., & Grunewald, P. (2018). Protecting data privacy is key to a smart energy future. *Nature Energy*, *3*(9), 702–704. https://doi.org/10.1038/s41560-018-0203-3

Wang, X., Smith, K., & Hyndman, R. (2006). Characteristic-Based Clustering for Time Series Data. *Data Mining and Knowledge Discovery*, *13*(3), 335–364. https://doi.org/10.1007/s10618-005-0039-x

Willinger, W., Paxson, V., Taqqu, M. S., & Willinger, W. (n.d.). *Self-Similarity and Heavy Tails: Structural Modeling of Network Tra c*. 26.

8. Appendix

The relationships between the time series features in the original data are shown in Figure 4.

- Spectral entropy distribution is skewed left, approximately 63% of series have a spectral entropy of at least 0.75 (a lot of series are already difficult to forecast).
- Spectral entropy is negatively correlated with features that improve forecastability such as Hurst exponent, strength of trend and seasonality, and remainder first autocorrelation coefficient (e-acf).
- Hurst is strongly correlated with strength of trend and seasonality
- Series with a larger mean tend to have higher variance

FIG 4 (Scatterplot matrix showing scatterplots between each feature pair, kernel density of each feature, and correlations between each feature pair for the original data.)

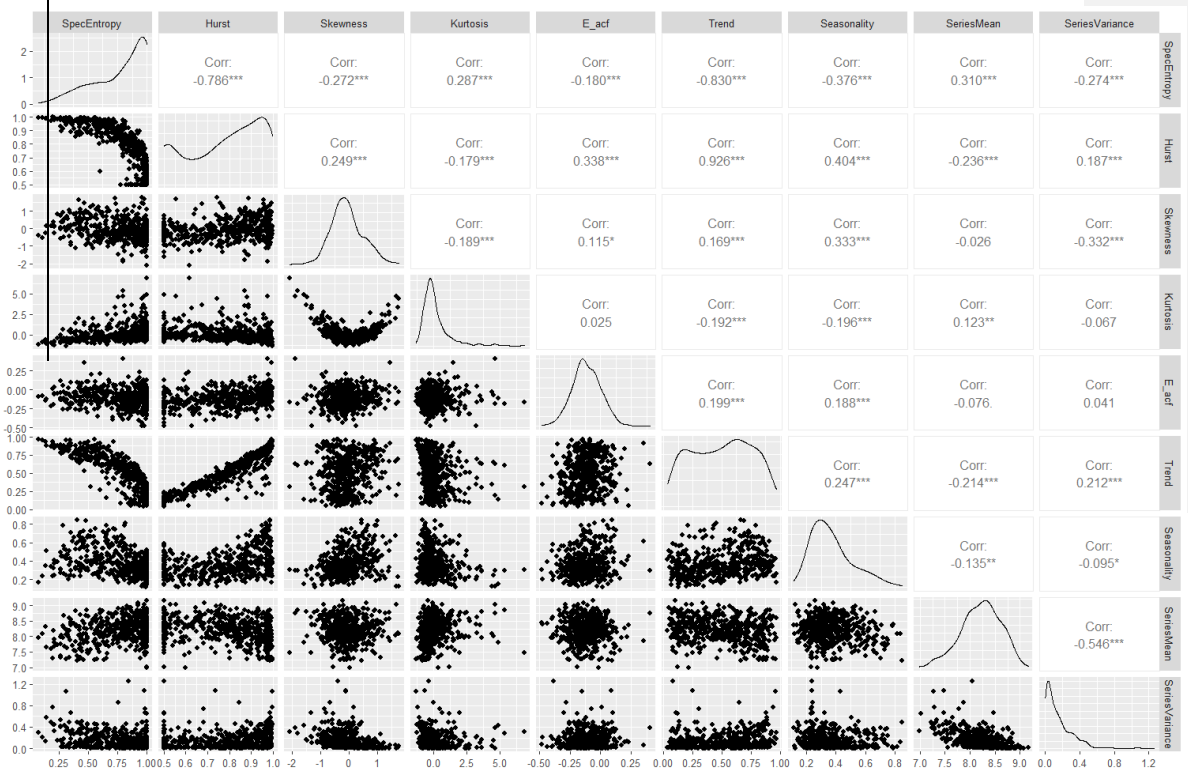

In the upper triangle of **FIG 4**, "***" denotes p-value < 0.001, "**" denotes p-value < 0.01, "*" denotes p-value < 0.05, "." denotes p-value < 0.10, "" is shown otherwise.

The Kullback-Leibler divergence between two probability densities $p(f)$ and $q(f)$ is defined as

$$\int_{\mathbb{R}^d} p(f) \log p(f)/q(f)\, df$$

where $p(f)$ is the probability density of the original feature, and the probability density of the feature from the protected data is denoted $q(f)$. Following the approach of (Spiliotis et al., 2020), we approximate $p(f)$ and $q(f)$ using normalized kernel densities, and estimate the KL-divergence between $p(f)$ and $q(f)$ as

$$KL(p,q) = \sum_f \hat{p}(f) log \frac{\hat{p}(f)}{\hat{q}(f)}.$$

Letting $H(p)$ denote the entropy of $p(f)$, the percentage difference between $p(f)$ and $q(f)$ is approximately

$$PD(p,q) = \frac{KL(p,q)}{H(p)} * 100.$$

Mathematical Details of Identification and Attribute Disclosure

To perform identification disclosure, we assume a third party possesses some original data pertaining to a unit of interest in the protected dataset. For the above example, this would be some sequence of original daily sales quantities for a known retailer. Denote this original data $\boldsymbol{c_i} = (ID_i, c_i)$, which contains a direct identifier ID_i (e.g., the identity of retailer i) and original data $c_i = (A_{i,t'}, \dots, A_{i,t'+E})$ which contains a sequence of values which are components of the original time series x_j.

We let M_i denote the random variable (from the perspective of the third party) that indicates the corresponding PID_j for ID_i, i.e., $M_i = j$ when the values in $\boldsymbol{c}_i$ are components of the original version of protected series j. Since the true value $M_i = j^*$ is unknown, the third party predicts the value of M_i to be the series j with the highest match probability, conditional on the known values, as follows

$$\widehat{M}_i = argmax_j P(M_i = j|c_i), \quad (1)$$

where identification disclosure occurs when $\widehat{M}_i = j^*$. The probability $P(M_i = j|c_i)$ is calculated as follows. Let $\tilde{x}_j = (P_{j,t'}, \dots, P_{j,t'+E}), j = 1, \dots, J$ denote the protected values of each time series j that occur in the same time periods as c_i. The third party computes the similarity between c_i and the protected values $\tilde{x}_j, j = 1, \dots, J$ using the Euclidean distance,

$$s(c_i, \tilde{x}_j) = \frac{1}{||c_i - \tilde{x}_j||_2}, j = 1, \dots, J.$$

Using these similarities the third party builds a probability mass function for M_i over all protected series in X' as

$$P(M\_i = j\ |c_i) = \frac{s(c_i, \tilde{x}_j)}{\sum_{j=1}^{N} s(c_i, \tilde{x}_j)},$$

and predicts $\widehat{M}_i$ as in (1).

To estimate the risk of identification disclosure, we perform simulations in which E sequential values are sampled from each original time series x_j, and we measure the average proportion of series which are identified. The sampled values are denoted $C = [\boldsymbol{c}_1, \dots, \boldsymbol{c}_J]^T$. Each of the vectors $\boldsymbol{c}_i$ corresponds to one of the J original time series and we compute r_j conditional on the sampled c_i from series j. We repeat this simulation S times to obtain $\boldsymbol{C} = \{C_1, \dots, C_S\}$, and compute the average proportion of correctly identified time series across all external data samples and original time series.

$$\bar{P} = \frac{1}{J * S} \sum_{s=1}^{S} \sum_{i=1}^{J} [\widehat{M}_i^s = j^*]$$

where [.] are Iverson brackets.

These simulations assume that the third party in possession of C predicts the match for each vector $\boldsymbol{c}_i$ independently of the predicted matches for other vectors. The risk estimate from a given

Commented [B24]: Membership inference paper

simulation is equivalent to the identification risk when J independent third parties are each in possession of one of the vectors $\boldsymbol{c}_i$ and each attempts identification risk as described above. Overall, multiple vectors may be matched to the same protected time series.

8.1. Privacy Assessment – Attribute Disclosure

To perform attribute disclosure, we assume the third party predicts additional original values for each protected time series based on the known values C and the predicted match $\widehat{M}_i, i = 1, \dots, J$ for each vector $\boldsymbol{c}_i$, as simulated above. For our purposes, we assume the third party is interested in the value $A_{j,t'+E+1}$ from each time series that immediately follows the known values $c_i = \left(A_{i,t'}, \dots, A_{i,t'+E}\right)$. The third party regresses the $J \times E$ known values in C on the corresponding protected values from each matched series,

$$A_{i,t'} \sim \beta_0 + \beta_1 P_{\widehat{M}_i,t'} + \epsilon \quad (1)$$

and predicts the unknown value of each time series in time period $t' + E + 1$ based on the protected value from that period,

$$\widehat{A_{i,t'+E+1}} = \beta_0 + \beta_1 P_{\widehat{M}_i,t'+E+1} \quad (2)$$

To estimate the risk of attribute disclosure in a protected dataset, i.e., the risk of the third party correctly predicting the value of each time series in time period $t' + E + 1$, we perform the regression and prediction steps (1) and (2) for each $C_s \in \boldsymbol{C}$, and measure the mean absolute error between the predicted and actual original values.

$$\bar{A} = \frac{1}{S * J} \sum_{s=1}^{S} \sum_{i=1}^{J} \left| \widehat{A^s_{i,t+E+1}} - A_{i,t+E+1} \right|$$